Resonance Raman Spectroscopy of Ribonucleotide Reductase. Evidence for a Deprotonated Tyrosyl Radical and Photochemistry of the Binuclear Iron Center†

Gabriele Backes,‡ Margareta Sahlin,§ Britt-Marie Sjöberg,§ Thomas M. Loehr,‡ and Joann Sanders-Loehr*,‡

Department of Chemical and Biological Sciences, Oregon Graduate Center, Beaverton, Oregon 97006-1999, and Department of Molecular Biology, University of Stockholm, S-10691 Stockholm, Sweden

Received August 16, 1988; Revised Manuscript Received October 20, 1988

ABSTRACT: Native ribonucleotide reductase from *Escherichia coli* exhibits a resonance-enhanced Raman mode at 1498 cm^{-1} that is characteristic of a tyrosyl radical. The Raman frequency as well as the absorption maximum at 410 nm identifies the radical as being in a deprotonated state. The B2 subunit of ribonucleotide reductase shows an additional resonance Raman mode at 493 cm^{-1} that has been assigned to the symmetric stretch of an Fe–O–Fe moiety. When samples of active B2 or metB2 are exposed to a tightly focused laser beam at 406.7 nm, there is a loss of intensity at 493 cm^{-1} and the appearance of a new peak at 595 cm^{-1}. Although the 595-cm^{-1} feature was previously assigned to an Fe–OH vibration on the basis of its 23-cm^{-1} shift to lower energy in $H_2{}^{18}O$ and the apparent dependence of its intensity on pH [Sjöberg, B. M., Loehr, T. M., & Sanders-Loehr, J. (1987) *Biochemistry 26*, 4242], the present studies indicate that the intensity of this mode is dependent primarily on input laser power. The peak at 595 cm^{-1} is more plausibly assigned to a new ν_s(Fe–O–Fe) mode in view of its lack of the deuterium isotope dependence expected for an Fe–OH mode and its resonant scattering cross section which is comparable to that of the 493-cm^{-1} mode. This new species has a calculated Fe–O–Fe angle of ~113° compared to ~138° calculated for the Fe–O–Fe unit in unmodified protein B2. One possible explanation for the photoinduced vibrational mode is that a bridging solvent molecule has been inserted in place of a bridging carboxylate.

Ribonucleotide reductase catalyzes the enzymatic formation of deoxyribonucleotides and, therefore, plays a pivotal role in DNA biosynthesis in all living organisms (Lammers & Follman, 1983). The enzyme from *Escherichia coli* is composed of two nonidentical subunits, B1 and B2 (Reichard & Ehrenberg, 1983). Protein B1 has a molecular weight of 170000 and contains two redox-active dithiol groups. Protein B2 has a molecular weight of 87000 and contains a stable organic free radical, which has been assigned to an oxidation product of a tyrosine residue of the protein. This radical is generated and stabilized by an adjacent dimeric iron center, both of which are essential for enzymatic activity (Sahlin et al., 1987; Larsson & Sjöberg, 1986). Treatment of native protein B2 (henceforth referred to as active B2)[1] with 1 equiv of reducing agent produces metB2, which has lost the radical but still contains an intact binuclear ferric site (Sahlin et al., 1988).

Binuclear iron cores are relevant units in proteins such as hemerythrin (Harrington & Wilkins, 1987), ribonucleotide reductase (Sjöberg & Gräslund, 1983), and purple acid phosphatase (Antanaitis & Aisen, 1983). The only structure determined by X-ray crystallography is for methemerythrin, where the two Fe(III) atoms are bridged by a solvent-derived oxo group and two protein carboxylates (Stenkamp et al., 1984).

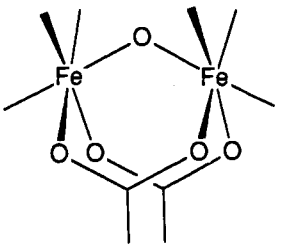

The additional ligands completing the octahedral environment are three histidines at one iron center and two histidines at the other. This arrangement leaves one vacant coordination site for the binding of exogenous ligands such as N_3^- in azidomethemerythrin or O_2 (as hydroperoxide) in the physiologically active oxyhemerythrin (Stenkamp et al., 1985; Kurtz et al., 1977; Shiemke et al., 1984).

As was observed earlier, the spectroscopic properties of the iron center in ribonucleotide reductase are remarkably similar to those of hemerythrin (Petersson et al., 1980). The presence of an oxo-bridged binuclear iron moiety in the reductase has been definitively established by resonance Raman spectroscopy (Sjöberg et al., 1982, 1987b) and by X-ray absorption spectroscopy (Bunker et al., 1987; Scarrow et al., 1986, 1987). The small Fe–O–Fe angle of ~135° and the short Fe···Fe distance of ~3.2 Å derived from the resonance Raman and EXAFS studies make it likely that ribonucleotide reductase contains

† This work was supported by the National Institutes of Health (GM 18865), the Swedish Medical Research Council (B86-03X-06801), and the Magnus Bergvall Foundation.

‡ Oregon Graduate Center.
§ University of Stockholm.

[1] Active B2 contains a tyrosyl free radical and an oxo-bridged binuclear Fe(III) center. MetB2 contains oxo-bridged binuclear Fe(III), but lacks the tyrosyl free radical. Reduced B2 contains a binuclear Fe(II) center and no tyrosyl free radical. ApoB2 lacks both iron and the tyrosyl free radical.

0006-2960/89/0428-1923$01.50/0

a multibridged structure with at least one μ-carboxylate ligand in addition to the μ-oxo group. At least one histidine ligand per iron has been implicated from NMR contact shifted resonances (Sahlin et al., 1986), and the strong Raman enhancement of the Fe–O–Fe vibrational intensity indicates that the histidines are positioned trans to the oxo bridge (Sjöberg et al., 1987b; Sanders-Loehr, 1988a).

In previous resonance Raman experiments on the metB2 subunit of ribonucleotide reductase, the Fe–O–Fe symmetric stretching vibration was identified as an intense feature at 492 cm^{-1}, which shifted 13 cm^{-1} to lower energy upon substitution of the bridging oxo group with ^{18}O (Sjöberg et al., 1982, 1987b). A weaker resonance-enhanced feature at $\sim$595 cm^{-1} was assigned as an Fe–OH vibration on the basis of its $\sim$ 23-cm^{-1} shift to lower energy upon incubation of B2 in $H_2{}^{18}O$ and its apparent similarity to the Fe–OH vibration at 565 cm^{-1} in hydroxymethemerythrin (Sjöberg et al., 1987b; Shiemke et al., 1986). However, a reevaluation of the assignment of the $\sim$595-cm^{-1} peak in ribonucleotide reductase has been necessitated by more critical experiments showing that its intensity is not affected by pH or D_2O but is strongly dependent on the nature of the laser illumination of the sample. This peak is more likely due to ν_s(Fe–O–Fe) of a modified binuclear iron cluster, most likely formed as a result of the photochemical dissociation or destruction of a carboxylate ligand.

Experimental Procedures

Samples. Proteins B1 and B2 were purified from separate overproducing *E. coli* strains carrying the recombinant plasmids pLSH1 (Larsson, 1984; Larsson et al., 1988) and pBS1 (Sjöberg et al., 1986), respectively. The mutant B2 protein containing Phe 122 in place of Tyr 122 was purified from an overproducing *E. coli* strain carrying the recombinant plasmid pAL83 (Larsson & Sjöberg, 1986). The radical-free form of protein B2 (metB2)[1] was obtained by incubating a concentrated sample of active B2 ($\sim$2 mM) in 0.05 M Tris-HCl (pH 7.6) with 100 mM hydroxyurea (Calbiochem) for 15 min at ambient temperature. Excess hydroxyurea was removed by diluting 10–20-fold with buffer and reconcentrating in a Centricon 30 filtration device (Amicon) at 4 °C for 1–2 h. This procedure was generally repeated two times or until the hydroxyurea concentration was $\leq$5 μM. Changes in sample buffer pH or isotopic composition were accomplished by a similar dilution and reconcentration procedure using 0.05 M Tris-HCl buffer. Deuterium or ^{18}O-enriched buffer was prepared by dissolving freeze-dried buffer in D_2O (99 atom %, Sigma) or $H_2{}^{18}O$ (97 atom %, YEDA).

Hydroxomethemerythrin from *Phascolopsis gouldii* was prepared as described previously (Shiemke et al., 1986). The Raman sample was 3.4 mM in binuclear iron sites in 0.2 M Tris–SO_4 (pH 8.5). The tribridged model, $[Fe_2O(Ac)_2(tacn)_2]I_2{\cdot}3H_2O{\cdot}{}^1/_2NaI$; tacn = triazacyclononane (Wieghardt et al., 1983) was the gift of Dr. Karl Wieghardt. The complex was dissolved in CH_3CN for Raman experiments.

Raman Spectroscopy. Raman spectra were collected on a computer-interfaced Jarrell-Ash spectrophotometer (Loehr et al., 1979) equipped with a Spectra-Physics 2025-11 Kr ion laser, a Coherent Innova 90-6 Ar ion laser, an RCA C31034A photomultiplier tube, and an ORTEC Model 9302 amplifier/discriminator. Excitation wavelengths were 363.8, 406.7, 413.1, and 457.9 nm. The majority of the experiments were performed by using 90° scattering from a sample capillary kept at a temperature of $\sim$293 K in the strong air flow from a 10-cm diameter muffin fan in the sample chamber. Two different kinds of lenses were employed for focusing purposes. For a diffuse laser beam, a cylindrical lens (which produces a line focus) was placed at its focal distance of 150 mm from the sample. For a tightly focused laser beam, a spherical lens (which produces a spot focus) was placed at its focal distance of 75 mm from the sample, and a 0.25 diopter lens was placed at an earlier point in the beam to control divergence. Low-temperature spectra were obtained by 150° backscattering from samples frozen at 15 K onto the gold-plated cold finger of a closed-cycle helium Displex (Air Products) or in a capillary at $\sim$90 K in a liquid N_2-cooled Dewar (Sjöberg et al., 1982). A cylindrical focusing lens was used for low-temperature work along with an Applied Photophysics fused silica prism monochromator to remove interfering laser plasma lines.

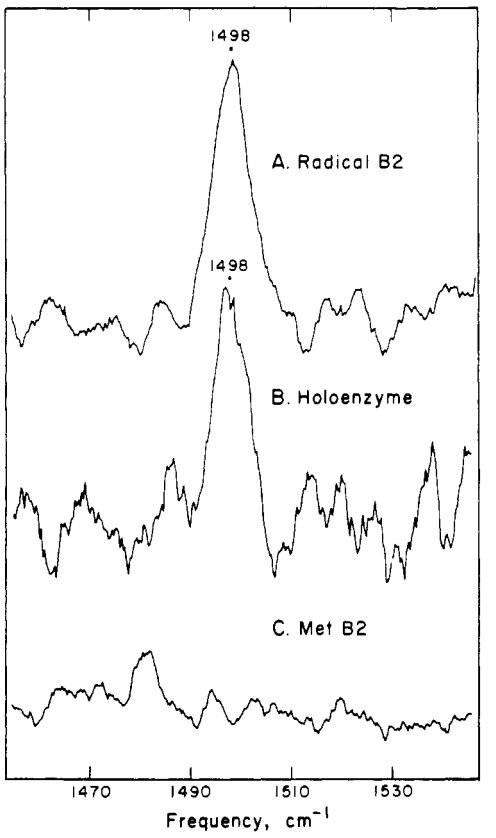

FIGURE 1: Resonance Raman spectra of tyrosyl radical moiety in (A) active B2 (1.8 mM, pH 8.0), (B) holoenzyme (0.64 mM in B1, 0.55 mM in B2, pH 8.0), and (C) metB2 (1.5 mM, pH 9.0). Spectra were recorded at 90 K with 406.7-nm excitation (6 mW), cylindrical lens, 7.0-cm^{-1} slit width, and 2.0 cm^{-1} s^{-1} scan rate and represent accumulations of 9, 9, and 18 scans, respectively.

Sample volumes were typically 10–15 μL and protein B2 concentrations were 1–2 mM in 0.05 M Tris buffer at pH 7.0–9.0. Anaerobic samples were prepared in capillaries sealed under a constant flow of argon. Isotope comparisons were performed on spectra collected sequentially under identical experimental conditions. Frequencies have been corrected by using an indene standard (Hendra & Loader, 1968) and are accurate to $\pm$1 cm^{-1}. Relative frequencies for isotope shifts were determined by curve fitting and are accurate to $\pm$0.5 cm^{-1}.

Results

Tyrosyl Radical in Protein B2 and Holoenzyme. In earlier Raman spectroscopic studies on the active B2 subunit[1] of ribonucleotide reductase at 90 K, there was some indication of a resonance-enhanced feature at $\sim$1500 cm^{-1} (Sjöberg et al., 1987b). A vibration at this frequency would be charac-

Table I: Resonance Raman Vibrational Frequencies for Various Forms of Ribonucleotide Reductase Subunits[a]

sample	ν_s(Fe–O–Fe)[b] (cm^{-1})		ν_s(Fe–O–Fe)$_p$[c] (cm^{-1})	
	H_2O	ΔD_2O	H_2O	ΔD_2O
metB2	493	+4	595	0
metB2 (Tyr 122 → Phe)	493	+4	595	
active B2	493[d]	+5[e]	595[d]	
holoenzyme (B1 + B2)[d]	493			

[a] Spectra obtained on samples in capillaries at ~293 K with 90° scattering. [b] Spectrum of the intact Fe–O–Fe cluster obtained with a diffuse laser beam. [c] Spectrum of the photoinduced Fe–O–Fe cluster, (Fe–O–Fe)$_p$, obtained with a focused laser beam. [d] Predominantly metB2 due to destruction of the radical during laser exposure at 293 K. [e] Spectrum of active B2 obtained at 90 K (Sjöberg et al., 1982).

teristic of a phenoxyl radical C–O vibrational mode (Tripathi & Schuler, 1984). A more careful analysis of protein B2 revealed a strongly enhanced peak at 1498 cm^{-1} (Figure 1A). Its assignment as the tyrosyl radical C–O stretch in active B2 was verified by the absence of this mode in the radical-free metB2 (Figure 1C). Reconstitution of the ribonucleotide reductase holoenzyme by recombination of B1 and B2 subunits caused very little perturbation of the B2 subunit. The tyrosyl radical vibration remained at 1498 cm^{-1} (Figure 1B), and the Fe–O–Fe symmetric stretch occurred at 493 cm^{-1} (Table I). These findings are in agreement with EPR data that show identical tyrosyl radical spectra for B2 alone and for the B1–B2 complex (Sahlin et al., 1987). The resonance Raman spectrum of active B2 in D_2O was indistinguishable from that obtained in H_2O, indicating either that the C–O moiety of the radical is not associated with a proton or that this site is inaccessible to proton exchange.

Phenylalanine 122 Mutant. Site-directed mutagenesis has been used to convert the conserved tyrosine at position 122 in the B2 polypeptide chain of ribonucleotide reductase to a phenylalanine (Larsson & Sjöberg, 1986). The resultant protein fails to exhibit any enzymatic activity, thus allowing Tyr 122 to be identified as the site of the tyrosyl free radical in the native enzyme. The optical spectrum of the mutant protein (Larsson et al., 1988) is similar to that of metB2 (Petersson et al., 1980), indicating the presence of an intact binuclear iron site. This has been verified by resonance Raman spectroscopy. The Fe–O–Fe symmetric stretch is observed at 493 cm^{-1} in both metB2 and the (Tyr 122 → Phe) mutant of protein B2 (Table I). Previous studies at 90 K showed identical Fe–O–Fe vibrational frequencies for the active and met forms of protein B2 (Sjöberg et al., 1982). A further similarity between the three species is the ~4-cm^{-1} shift of ν_s (Fe–O–Fe) to higher energy in D_2O (Table I). This deuterium isotope effect has been ascribed to hydrogen bonding between a protein component and the bridging oxo group (Sjöberg et al., 1987). Thus, it appears that the conversion of Tyr 122 to Phe 122 has not altered the geometry of the Fe–O–Fe moiety or its hydrogen-bonding interactions with the protein. These observations also exclude Tyr 122 from being the hydrogen-bond donor to the Fe–O–Fe group.

Photochemistry of the B2 Subunit. Previous resonance Raman experiments on the metB2 protein of ribonucleotide reductase were performed on samples in capillaries maintained at 278 K in an ice-filled Dewar (Sjöberg et al., 1987). The design of the Dewar (Sjöberg et al., 1982) necessitated the use of ~150° backscattering geometry and a cylindrical lens that results in a rather diffuse beam impinging on the sample. Under these conditions, ^{18}O-sensitive vibrational modes were observed at 492 and ~595 cm^{-1} in an intensity ratio of ~4:1, respectively. We have now obtained similar results for metB2

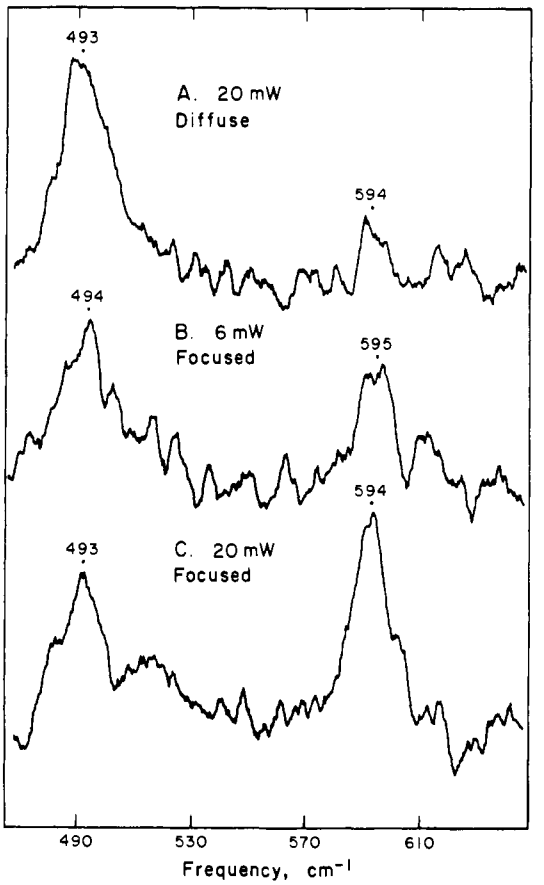

FIGURE 2: Resonance Raman spectra of metB2 obtained with 406.7-nm excitation under different laser conditions: (A) 20 mW, diffuse focus using cylindrical lens (1.5 mM protein, pH 9.0); (B) 6 mW, tight focus using spherical lenses (2 mM protein, pH 7.0); (C) 20 mW, tight focus using spherical lenses (2 mM protein, pH 7.0). Data were obtained at ~293 K at a scan rate of 1.0 cm^{-1} s^{-1} and a slit width of 7 cm^{-1}. Spectra have been subjected to background subtraction and a 25-point third-order polynomial smoothing function (Loehr et al., 1979); they represent accumulations of 10, 3, and 3 scans, respectively.

samples at 15 K using 150° backscattering and at room temperature in a capillary using 90° scattering (Figure 2A), provided that the incident laser beam was diffused by passage through a cylindrical focusing lens. However, a marked spectral change occurred when samples in bare capillaries in a 90°-scattering geometry were subjected to a 406.7-nm laser beam tightly focused through a spherical lens. Under these conditions there was a substantial increase in the intensity of the peak at 595 cm^{-1} relative to the ν_s(Fe–O–Fe) peak at 493 cm^{-1} (Figure 2C). Quantitation of these vibrational features relative to the 1000-cm^{-1} phenylalanine mode of the protein showed an absolute increase in intensity at 595 cm^{-1} and a corresponding decrease in intensity at 493 cm^{-1} when compared to spectra taken under more diffuse illumination conditions. The extent of the reaction was dependent on excitation wavelength. When 457.9-nm excitation (30 mW) was used instead of 406.7 nm, only the 493-cm^{-1} peak was apparent with no discernible feature at 595 cm^{-1}.

Under focused beam conditions, the relative intensities of the 493- and 595-cm^{-1} components could be varied by changing the laser power. At 6-mW power the 493-cm^{-1} peak was still the dominant spectral feature (Figure 2B), whereas at 20-mW power the intensity at 595 cm^{-1} exceeded that at 493 cm^{-1} (Figure 2C). The photoinduced conversion of the 493-cm^{-1} species to the 595-cm^{-1} species did not appear to be a reversible process. Decreasing the laser power to 6 mW at any stage

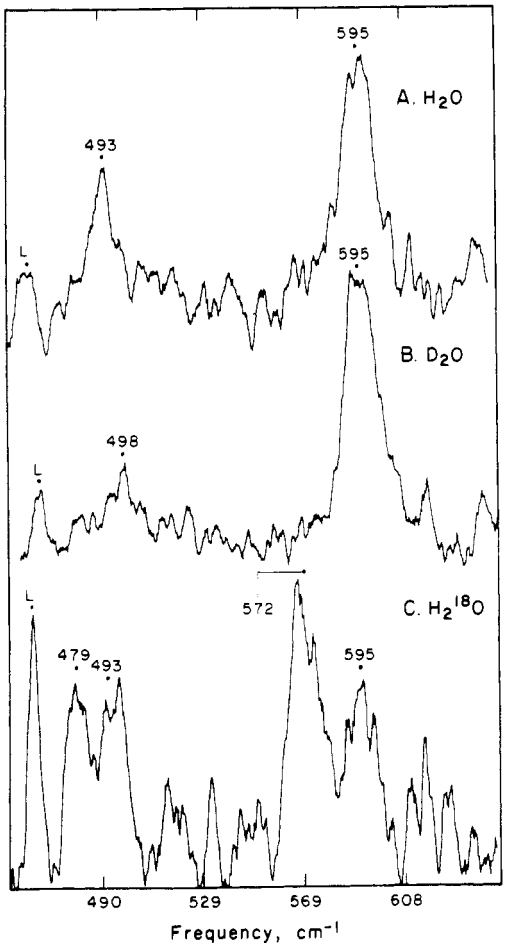

FIGURE 3: Resonance Raman spectra of metB2 in solvents of different isotopic composition: (A) 2.5 mM protein (pH 7.6) in H_2O; (B) 1.5 mM protein (pH 7.6) in D_2O; (C) 1.4 mM protein (pH 7.6) in 80% $H_2{}^{18}O$, 20% $H_2{}^{16}O$. Spectral conditions as in Figure 2C for 9, 9, and 12 scans, respectively. L denotes laser plasma line.

of the reaction did not result in a return to the relative intensities observed in the initial low-power spectrum (Figure 2B). Furthermore, the relative intensity at 595 cm^{-1} did not increase as rapidly as the increase in laser power (i.e., a 3–4-fold increase in laser power gave only a 1.3–1.5-fold increase in intensity). In addition, there was no buildup of the 595-cm^{-1} product with time (i.e., between 10 s and 30 min). These results indicate that there may be a fraction of the sample which is readily converted at low powers and another fraction which is more resistant to the photoreaction and requires considerably higher powers for conversion.

Incubation of metB2 in $H_2{}^{18}O$ under focused conditions resulted in the same oxygen isotope dependence as observed previously under nonfocused conditions (Sjöberg et al., 1987). The Fe–O–Fe vibration at 493 cm^{-1} underwent an ~14-cm^{-1} shift to lower energy, whereas the 595-cm^{-1} peak shifted down by 23 cm^{-1} to appear at 572 cm^{-1} (Figure 3A,C). In the deuterium-exposed sample, the 493-cm^{-1} peak exhibited the expected 5-cm^{-1} increase in frequency (Figure 3B). No such deuterium isotope dependence was observed for the 595-cm^{-1} peak. However, conversion of the 493-cm^{-1} moiety to the 595-cm^{-1} moiety was considerably more complete in D_2O than in H_2O, implying that the strength of hydrogen bonding of ligands in the binuclear iron cluster may alter the fraction of molecules that is photoreactive.

The absence of a frequency shift for the 595-cm^{-1} peak in the deuterium-exchanged protein in the present data is in conflict with our earlier report of a 2-cm^{-1} downshift in D_2O

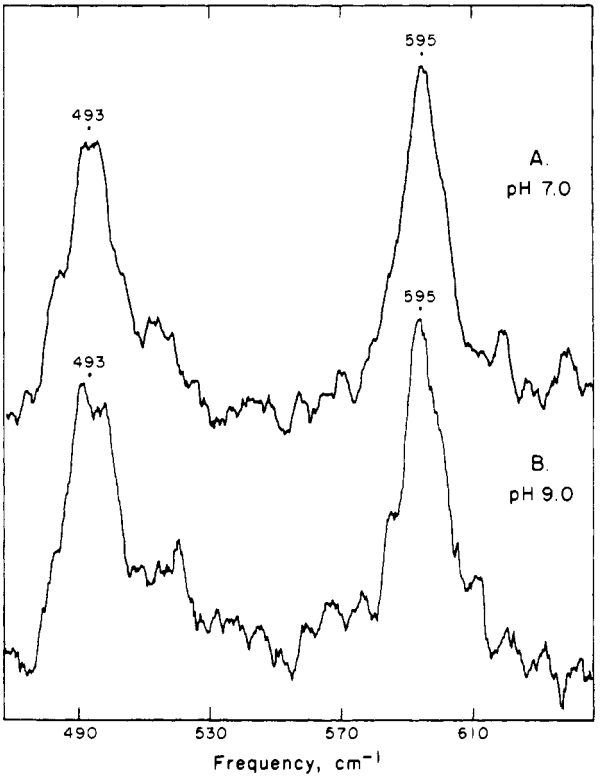

FIGURE 4: Resonance Raman spectra of metB2 at (A) pH 7.0 (1.5 mM protein) and (B) pH 9.0 (1.5 mM protein). Spectral conditions as in Figure 2C for 6 and 9 scans, respectively.

(Sjöberg et al., 1987b). The earlier observation was apparently incorrect and is attributable to the low peak intensities in those spectra, placing such frequency shifts within the limits of experimental error. The previously reported decrease in the 595-cm^{-1} peak intensity with decreasing pH was also incorrect, possibly due to slightly different laser focusing at the two pHs. A more careful investigation using tightly focused conditions now shows essentially identical relative peak intensities between pH 7.0 and 9.0 (Figure 4).

The lack of pH and deuterium dependence in the 595-cm^{-1} peak makes it doubtful that this feature is the Fe–OH vibration that we suggested earlier (Sjöberg et al., 1987b). The distinct oxygen isotope dependence and the appearance of intensity comparable to that of the 493-cm^{-1} peak obtained with low laser power make it more plausible to assign the 595-cm^{-1} peak to another symmetric Fe–O–Fe stretching mode. The increase in vibrational frequency is indicative of a decreased Fe–O–Fe bond angle in this photochemically altered binuclear iron cluster. Supporting evidence for such a change in bond angle would be the observation of an asymmetric Fe–O–Fe vibration at lower energy (Wing & Callahan, 1969) than the ν_{as} (Fe–O–Fe) located previously at ~756 cm^{-1} in radical-free B2 (Sjöberg et al., 1987b). Unfortunately, the poorer signal-to-noise in these strongly irradiated samples has prevented detection of the asymmetric stretching mode, which typically has low Raman intensity.

To learn more about the nature of the photoinduced process and the substrates involved, Raman spectra were obtained on samples prepared in an argon atmosphere and sealed in capillaries. Under focused-beam conditions, both active B2 and metB2 samples exhibited a peak at 595 cm^{-1} of about equal intensity to the peak at 493 cm^{-1}. This behavior is similar to that observed for aerobic samples (e.g., Figure 4). In previous experiments with metB2 it was found that deuterium-exchanged protein converts more efficiently to photoproduct

Table II: Properties of Oxo-Bridged Binuclear Iron Centers

sample	Fe–O–Fe angle obs[a]	Fe–O–Fe angle calc[b]	ν_s(Fe–O–Fe)[c] (cm^{-1}) ν_s	$\Delta\nu_s$ in ^{18}O
monobridged complexes				
$[Fe_2O(hedta)_2]^{2-}$	165	167	423	−2
$[Fe_2O(phen)_4(H_2O)_2]^{4+}$	155	156	395	−5
dibridged complex				
$[Fe_2O(OBz)(L)_2]^{+}$	129	124	494	−17
tribridged complexes				
azidomethemerythrin	135	136	507	−14
$Fe_2O(Ac)_2(HBpz_3)_2$	124	128	528	−17
$[Fe_2O(Ac)_2(tpbn)]_2^{4+}$	121		547	
$[Fe_2O(Ac)_2(tacn)_2]^{2+}$	119	130	540	−17
ribonucleotide reductase				
metB2	130	138	493	−13
metB2*		113	595	−23

[a] From X-ray crystallography for the following complexes: hedta (Lippard et al., 1967); phen (Plowman et al., 1984); dibridged with benzoate, L = *N*-(*O*-hydroxybenzyl)-*N*,*N*-bis(2-pyridylmethyl)amine (Yan et al., 1988); $HBpz_3$ (Armstrong et al., 1984); tpbn (Toftlund et al., 1986); tacn (Wieghardt et al., 1983); azidomethemerythrin (Stenkamp et al., 1984). From X-ray absorption spectroscopy for protein B2 (Scarrow et al., 1987). [b] Calculated from $\nu_s(Fe-^{16}O-Fe)$ and $\nu_s(Fe-^{18}O-Fe)$ according to the secular equation of Wing and Callahan (1969). [c] Values for ν_s and $\Delta\nu_s$ in cm^{-1} from resonance Raman spectroscopy for the following complexes: hedta and tpbn (W. D. Wheeler, A. K. Shiemke, B. A. Averill, T. M. Loehr, and J. Sanders-Loehr, unpublished results); phen (Plowman et al., 1984); $HBpz_3$ (Armstrong et al., 1984); tacn (Spool et al., 1985); azidomethemerythrin (Shiemke et al., 1984); metB2 (Sjöberg et al., 1987a); photochemically modified metB2* and dibridged complex (this work).

(Figure 3B). Anaerobic and aerobic samples of active B2 in D_2O gave similar spectra, both showing ~4-fold greater intensity at 595 cm^{-1} than at 493 cm^{-1}. These experiments demonstrate that O_2 has no apparent effect on the photochemical production of the new chromophoric Fe–O–Fe species $(Fe–O–Fe)_p$. Thus, the reaction is unlikely to involve a change in iron oxidation state.

A major difference between the Phe 122 mutant and the wild-type proteins is in their ability to form the photochemically induced $(Fe–O–Fe)_p$ structure. When the mutant protein was exposed to a focused beam, there was a considerably longer persistence of the 493-cm^{-1} peak and very little conversion to the 595-cm^{-1} species; however, a small feature amounting to ~10% of the intensity at 493 cm^{-1} was observed at 595 cm^{-1} after prolonged laser exposure. These results suggest that Tyr 122 in metB2 is somehow involved in the photochemical reaction, either directly or via some effect on protein conformation in the vicinity of the binuclear iron site.

Experiments on other binuclear-iron-containing complexes, hydroxomethemerythrin (Shiemke et al., 1986), the tribridged model complex $[Fe_2O(Ac)_2(tacn)_2]^{2+}$ (Spool et al., 1985), and the dibridged model complex $[Fe_2O(OBz)L_2]^{+}$ (Yan et al., 1988), reveal behavior closer to that of the Phe 122 mutant than of the wild-type B2 protein. In each case under focused-beam conditions there was a gradual disappearance of the ν_s(Fe–O–Fe) mode listed in Table II. However, this loss was not accompanied by the appearance of any new spectral components at higher or lower energy. Thus, the ability to form a stable $(Fe–O–Fe)_p$ species depends on the environment of the metal cluster and is not a general property of all multiply bridged binuclear iron centers. The azide and thiocyanate adducts of the monomeric muscle protein myohemerythrin do undergo a photochemical reaction that results in exchange of the bridging oxo group with solvent oxygen (Duff et al., 1981). Since the vibrational spectra of the products indicate no change in Fe–O–Fe angle, it is likely that the myohemerythrin reaction involves the photochemical dissociation and subsequent reformation of an Fe–μ-oxo bond rather than bonds to endogenous protein ligands.

Discussion

Tyrosyl Radical. Previous studies of the tyrosyl radical of protein B2 by electronic and EPR spectroscopy have identified it as a one-electron oxidized species with radical spin density localized on C-1, C-3, and C-5 of the aromatic ring (Sjöberg et al., 1978; Petersson et al., 1980). Although the EPR hyperfine splittings are similar to those of both protonated and deprotonated aryloxy radicals, the better match with the former led to the suggestion that the tyrosyl radical in protein B2 has a protonated hydroxyl group (Sjöberg et al., 1978). However, electronic and vibrational spectra of phenoxyl radicals are considerably more sensitive indicators of the protonation state. The resonance-enhanced mode at 1498 cm^{-1} in active B2 corresponds closely to the ν(C–O) modes observed for the deprotonated phenoxyl radical at 1505 cm^{-1} (Tripathi & Schuler, 1984) and for the deprotonated 4-hydroxyphenoxyl radical at 1515 cm^{-1} (Tripathi & Schuler, 1987). Protonation is expected to cause a substantial decrease in ν(C–OH), as is the case for phenol at 1249 cm^{-1} compared to phenolate at 1281 cm^{-1} (Pinchas, 1972). A similar trend is observed for the protonated 4-hydroxyphenoxyl radical with its ν(C–OH) at 1426 cm^{-1} (Tripathi & Schuler, 1987). Protonated phenols also show significant changes of 4–5 cm^{-1} for ν(C–OH) in D_2O (Jakobsen, 1965), and no such deuterium effect was observed in the case of the active B2 protein.

Further evidence in support of a deprotonated tyrosyl radical in ribonucleotide reductase is the fact that phenoxyl radical protonation generally occurs at very low pH (i.e., below pH 0) and results in a shift in the absorption maximum from ~410 nm in the deprotonated form to ~425 nm in the protonated form (Tripathi & Schuler, 1987). The 410-nm absorption maximum and the attendant vibrational progression to higher energy in the electronic spectrum of protein B2 (Petersson et al., 1980) are closely matched by the 400-nm absorption maximum and vibrational progession of the deprotonated phenoxyl radical (Tripathi & Schuler, 1984). A deprotonated tyrosyl radical in ribonucleotide reductase was proposed previously to explain the specific removal and replacement of a hydrogen atom from the C-3 position of ribose during the enzymatic reaction (Ashley & Stubbe, 1985; Salowe et al., 1987).

Photochemistry of the B2 Subunit. The new feature at 595 cm^{-1} that appears upon exposure of protein B2 to focused laser irradiation can be assigned to an Fe–O–Fe symmetric stretch on the basis of the following criteria. It is strongly resonance-enhanced with near-UV excitation, as is typical for oxo-bridged iron complexes that have intense oxo → Fe(III) CT bands in this spectral region (Sanders-Loehr, 1988a). It undergoes a 23-cm^{-1} shift to lower energy in the presence of $H_2{}^{18}O$, showing that it contains an oxygen derived from solvent. The vibrational frequency is unaffected by D_2O solvent or by changing the pH between 7 and 9, indicating that the Fe–O moiety is not a protonated species. The frequency is within the expected range for a ν_s(Fe–O–Fe) mode (Table II).

The increase in vibrational frequency from 493 to 595 cm^{-1} as well as the increase in oxygen isotope shift, $\Delta\nu_s$, from −13 to −23 cm^{-1} in going from ν_s(Fe–O–Fe) to $\nu_s(Fe–O–Fe)_p$ implies a significant change in structure at the binuclear iron site. As can be seen in Table II, vibrational frequencies are inversely proportional to the Fe–O–Fe angle. Larger Fe–O–Fe angles of 150–180° are characteristic of monobridged complexes and

give rise to low values for ν_s (i.e., <450 cm^{-1}) and $\Delta\nu_s$ (i.e., −2 to −5 cm^{-1}). The tribridged complexes with their smaller Fe–O–Fe angles of 120–140° have correspondingly larger values for ν_s (i.e., 490–550 cm^{-1}) and $\Delta\nu_s$ (i.e., −13 to −17 cm^{-1}). Calculations of Fe–O–Fe angles based on vibrational data agree fairly well with values determined by X-ray crystallography (Table II). The calculated Fe–O–Fe angle of 138 ± 5° for protein B2 is at the wide extreme for a μ-oxo, μ-carboxylato structure. The corresponding data for the photochemically modified protein, B2*, result in a calculated Fe–O–Fe angle of 113°, which is more acute than has yet been observed for a bridged μ-oxo binuclear iron complex.

It is of interest to determine the structural basis for the marked rearrangement of the Fe–O–Fe center in protein B2*. Transition metal complexes are capable of undergoing a variety of photochemical reactions, the most common of which are (1) production of an excited electronic state that is stable enough to be chemically characterized, (2) a photoredox process that alters the oxidation states of both metal and ligand, and (3) a photosubstitution reaction that involves ligand dissociation and replacement, most typically by aquation (Porterfield, 1984; Kutal & Adamson, 1987). Studies on ruthenium, iron, and manganese complexes have shown that these transition metals can form excited electronic states that are sufficiently populated to be probed by resonance Raman spectroscopy (Woodruff, 1983; Perng & Zink, 1988). However, such experiments require the high-power density of a pulsed laser to achieve conditions close to saturation of the excited state. It is unlikely that the low power CW laser excitation used in the present experiments could have produced enough excited-state molecules to account for the observed 50–100% conversion of protein B2 to protein B2*.

Of the remaining two processes, photoreduction of high-spin Fe(III) has been more strongly documented than photosubstitution (Balzani & Carassiti, 1974). Although the former would better explain the lack of reversibility of the protein B2 reaction, the lack of any dependence on molecular oxygen makes it questionable that an Fe-related photoredox process is occurring. A one-electron-reduced binuclear iron center would be expected as the stable product in the absence of O_2. Such an Fe(II)–Fe(III) species (typically, hydroxobridged) has not yet been observed for ribonucleotide reductase, and where it has been observed, as in semimethemerythrin, it has not yet revealed any resonance-enhanced modes associated with the Fe–OH–Fe moiety (Irwin et al., 1983). Since the observable photoproduct is believed to be an Fe(III)–O–Fe(III) species, any Fe(II) generated in a photoredox reaction would have to be reoxidized by some other protein component.

The most probable explanation is that the binuclear iron center in ribonucleotide reductase is undergoing a substitution reaction via photoinduced dissociation of one of the iron ligands and its replacement by a different incoming ligand. Although photodissociation of the bridging oxo group has been detected in azidometmyohemerythrin (Duff et al., 1981), this process is unlikely to explain the formation of protein B2* that appears to contain an intact Fe–O–Fe moiety. The change in Fe–O–Fe angle indicated in Table II would correspond to a decrease in iron–iron distance from 3.3 Å in protein B2 to 3.0 Å in protein B2*. The μ-oxo-bridged binuclear iron complexes listed in Table II with either one or two bridging carboxylates have Fe···Fe distances in the range 3.19–3.24 Å. Shorter Fe···Fe distances of 3.08–3.12 Å are more characteristic of $Fe_2(OH)_2$ species with two monoatomic bridges (Thich et al., 1981). These observations suggest that a bridging carboxylate ligand in protein B2 may have been dissociated and replaced by a bridging solvent molecule in protein B2*. Such a binuclear center in protein B2* would be reminiscent of the μ-oxo, μ-aquo structure proposed for the binuclear complex of Cu(II)(Me-tacn) (Chaudhuri et al., 1985). This raises the possibility that protein B2 originally contained a dibridged rather than a tribridged iron center. Alternatively, the formation of protein B2* may result directly from the photodissociation of a bridging or terminal ligand (other than the μ-oxo group) which concomitantly distorts the geometry of the entire metal cluster.

The wavelength dependence of the photochemical reaction also suggests that a ligand other than the μ-oxo group is involved in the photodissociation process. Resonance enhancement of the 493-cm^{-1} Fe–O–Fe mode is driven by excitation within the μ-oxo → Fe(III) CT band. Such enhancement can be observed with 457.9-nm excitation and increases substantially with 413.1 nm. In contrast, the production of $(Fe–O–Fe)_p$ is only observed with 413.1 or 406.7 nm. This implies that the latter process is being driven by a different ligand → Fe(III) CT transition whose absorption maximum lies farther into the UV region.

Structure of the Binuclear Iron Site. Although the binuclear iron center in protein B2 appears to have a multibridged structure analogous to that in hemerythrin, the nature and number of bridging and terminal ligands remains to be determined. At least one histidine per iron has been implicated by NMR studies (Sahlin et al., 1986) and by the extent of resonance Raman enhancement of the Fe–O–Fe vibration, which suggests unsaturated nitrogen ligands trans to the oxo group (Sjöberg et al., 1987b; Sanders-Loehr, 1988a). The similar intensity of the $(Fe–O–Fe)_p$ symmetric stretch in the photochemically modified protein indicates the continued presence of histidine ligands trans to the oxo group. Comparison of the EXAFS of hemerythrin and protein B2 leads to the conclusion that there are fewer histidine ligands per iron in protein B2 and that the other ligands are oxygen donors (Bunker et al., 1987; Scarrow et al., 1986, 1987). Suitable candidates for the latter include protein-derived carboxylates and solvent-derived aquo or hydroxo species. Although a hydroxide ligand was specifically proposed on the basis of our previous resonance Raman studies (Sjöberg et al., 1987b), our present work shows that the spectrum was misassigned and that there is no longer any unambiguous evidence for such a ligand.

The fact that O_2 can serve as an oxidant of the binuclear iron center makes it likely that there is at least one exogenous ligand binding site in the cluster. This site could actually be vacant, yielding a 5-coordinate iron as in methemerythrin (Stenkamp et al., 1984), or it could contain a replaceable solvent molecule. However, this site must be less accessible to anions (e.g., N_3^-, CN^-) than the corresponding site in methemerythrin since the binuclear iron cluster in protein B2 has never been observed to bind exogenous anionic ligands. The reaction of reduced protein $B2^1$ with O_2 that generates the tyrosyl radical could proceed via the formation of a hydroperoxide intermediate in a manner analogous to the reaction of deoxyhemerythrin plus O_2 (Sanders-Loehr, 1988b). Since the B2 subunit is composed of two identical polypeptide chains, the random binding of O_2 to one of the two iron atoms could explain the generation of only one tyrosyl radical per B2 subunit and thereby account for the half-of-sites reactivity (Sjöberg et al., 1987a).

ACKNOWLEDGMENTS

We are grateful to Dr. Robert H. Schuler for helpful discussions on the identification of phenoxyl radicals and to Drs.

Karl Wieghardt, Hans Toftlund, and Lawrence Que, Jr., for providing us with samples of the tribridged tacn, tribridged tpbn and dibridged μ-benzoate complexes, respectively.

Registry No. Fe, 7439-89-6; ribonucleotide reductase, 9047-64-7; tyrosyl radical, 16978-66-8.

REFERENCES

Antanaitis, B. C., & Aisen, P. (1983) *Adv. Inorg. Biochem. 5*, 111.

Armstrong, W. H., Spool, A., Papaefthymiou, G. C., Frankel, R. B., & Lippard, S. J. (1984) *J. Am. Chem. Soc. 106*, 3653.

Ashley, G. W., & Stubbe, J. (1985) *Pharmacol. Ther. 30*, 301.

Balzani, V., & Carassiti, V. (1974) *Photochemistry of Coordination Compounds*, pp 161–192, Academic Press, London.

Bunker, G., Petersson, L., Sjöberg, B.-M., Sahlin, M., Chance, M., Chance, B., & Ehrenberg, A. (1987) *Biochemistry 26*, 4708.

Chaudhuri, P., Ventur, D., Wieghardt, K., Peters, E.-M., Peters, K., & Simon, A. (1985) *Angew. Chem., Int. Ed. Engl. 24*, 57.

Duff, L. L., Klippenstein, G. L., Shriver, D. F., & Klotz, I. M. (1981) *Proc. Natl. Acad. Sci. U.S.A. 78*, 4138.

Harrington, P. C., & Wilkins, R. G. (1987) *Coord. Chem. Rev. 79*, 195.

Hendra, P. J., & Loader, E. J. (1968) *Chem. Ind., 718*.

Irwin, M. J., Duff, L. L., Shriver, D. F., & Klotz, I. M. (1983) *Arch. Biochem. Biophys. 224*, 473.

Jakobsen, R. J. (1965) *Spectrochim. Acta 21*, 433.

Kurtz, D. M., Jr., Shriver, D. F., & Klotz, I. M. (1977) *Coord. Chem. Rev. 24*, 145.

Kutal, C., & Adamson, A. N. (1987) in *Comprehensive Coordination Chemistry* (Wilkinson, G., Gillard, R. D., & McCleverty, J. A., Eds.) Vol. 1, pp 385–414, Pergamon, Oxford, U.K.

Lammers, M., & Follmann, H. (1983) *Struct. Bonding (Berlin) 54*, 27.

Larsson, Å. (1984) *Acta Chem. Scand. B38*, 905.

Larsson, Å., & Sjöberg, B.-M. (1986) *EMBO J. 5*, 2037.

Larsson, Å., Karlsson, M., & Sjöberg, B.-M. (1988) (submitted for publication).

Lippard, S. J., Schugar, H., & Walling, C. (1967) *Inorg. Chem. 6*, 1825.

Loehr, T. M., Keyes, W. E., & Pincus, P. A. (1979) *Anal. Biochem. 96*, 456.

Perng, J.-H., & Zink, J. I. (1988) *Inorg. Chem. 27*, 1403.

Petersson, L., Gräslund, A., Ehrenberg, A., Sjöberg, B.-M., & Reichard, P. (1980) *J. Biol. Chem. 255*, 6706.

Pinchas, S. (1972) *Spectrochim. Acta 28A*, 801.

Plowman, J. E., Loehr, T. M., Schauer, C. K., & Anderson, O. P. (1984) *Inorg. Chem. 23*, 3553.

Porterfield, W. W. (1984) *Inorganic Chemistry* pp 636–651, Addison-Wesley, Reading, MA.

Reichard, P., & Ehrenberg, A. (1984) *Science 221*, 514.

Sahlin, M., Ehrenberg, A., Gräslund, A., & Sjöberg, B.-M. (1986) *J. Biol. Chem. 261*, 2778.

Sahlin, M., Ehrenberg, A., Gräslund, A., Petersson, L., Sjöberg, B.-M., & Thelander, L. (1987) *Biochemistry 26*, 5541.

Sahlin, M., Gräslund, A., Petersson, L., Ehrenberg, A., & Sjöberg, B.-M. (1988) *Biochemistry* (in press).

Salowe, S. P., Ator, M. A., & Stubbe, J. (1987) *Biochemistry 26*, 3408.

Sanders-Loehr, J. (1988a) in *Metal Clusters in Proteins* (Que, L., Jr., Ed.) pp 49–67, American Chemical Society, Washington, DC.

Sanders-Loehr, J. (1988b) in *Oxidases and Related Redox Systems* (Mason, H. S., King, T. E., & Morrison, M., Eds.) pp 193–209, Liss, New York.

Scarrow, R. C., Maroney, M. J., Palmer, S. M., Que, L., Jr., Salowe, S. P., & Stubbe, J. A. (1986) *J. Am. Chem. Soc. 108*, 6832.

Scarrow, R. C., Maroney, M. J., Palmer, S. M., Que, L., Jr., Roe, A. L., Salowe, S. P., & Stubbe, J. A. (1987) *J. Am. Chem. Soc. 109*, 7857.

Shiemke, A. K., Loehr, T. M., & Sanders-Loehr, J. (1984) *J. Am. Chem. Soc. 106*, 4951.

Shiemke, A. K., Loehr, T. M., & Sanders-Loehr, J. (1986) *J. Am. Chem. Soc. 108*, 2437.

Sjöberg, B.-M., & Gräslund, A. (1983) *Adv. Inorg. Biochem. 5*, 87.

Sjöberg, B.-M., Reichard, P., Gräslund, A., & Ehrenberg, A. (1978) *J. Biol. Chem. 253*, 6863.

Sjöberg, B.-M., Loehr, T. M., & Sanders-Loehr, J. (1982) *Biochemistry 21*, 96.

Sjöberg, B.-M., Hahne, S., Karlsson, M., Jörnvall, H., Göransson, M., & Uhlin, B.-E. (1986) *J. Biol. Chem. 261*, 5658.

Sjöberg, B.-M., Karlsson, M., & Jörnvall, H. (1987a) *J. Biol. Chem. 262*, 9736.

Sjöberg, B.-M., Sanders-Loehr, J., & Loehr, T. M. (1987b) *Biochemistry 26*, 4242.

Spool, A., Williams, I. D., & Lippard, S. J. (1985) *Inorg. Chem. 24*, 2156.

Stenkamp, R. E., Sieker, L. C., & Jensen, L. H. (1984) *J. Am. Chem. Soc. 106*, 618.

Stenkamp, R. E., Sieker, L. C., Jensen, L. H., McCallum, J. D., & Sanders-Loehr, J. (1985) *Proc. Natl. Acad. Sci. U.S.A. 82*, 713.

Thich, J. A., Toby, B. H., Powers, D. A., Potenza, J. A., & Schugar, H. J. (1981) *Inorg. Chem. 20*, 3314.

Toftlund, H., Murray, K. S., Zwack, P. R., Taylor, L. F., & Anderson, O. P. (1986) *J. Chem. Soc., Chem. Commun.*, 191.

Tripathi, G. N. R., & Schuler, R. H. (1984) *J. Chem. Phys. 81*, 113.

Tripathi, G. N. R., & Schuler, R. H. (1987) *J. Phys. Chem. 91*, 5881.

Wieghardt, K., Pohl, K., & Gebert, W. (1983) *Angew. Chem., Int. Ed. Engl. 22*, 727.

Wing, R. M., & Callahan, K. P. (1969) *Inorg. Chem. 8*, 871.

Woodruff, W. H. (1983) in *Inorganic Chemistry: Toward the 21st Century* (Chisholm, M. H., Ed.) pp 473–508, American Chemical Society, Washington, DC.

Yan, S., Que, L., Jr., Taylor, L. F., & Anderson, O. P. (1988) *J. Am. Chem. Soc. 110*, 5222.